AIP | Journal of Applied Physics

# Characteristics of electric-field-induced polarization rotation in 001-poled Pb(Mg1/3Nb2/3)O3-PbTiO3 single crystals close to the morphotropic phase boundary

J. Peräntie, J. Hagberg, A. Uusimäki, J. Tian, and P. Han

Citation: J. Appl. Phys. **112**, 034117 (2012); doi: 10.1063/1.4745902
View online: http://dx.doi.org/10.1063/1.4745902
View Table of Contents: http://jap.aip.org/resource/1/JAPIAU/v112/i3
Published by the AIP Publishing LLC.

# Characteristics of electric-field-induced polarization rotation in ⟨001⟩-poled $Pb(Mg_{1/3}Nb_{2/3})O_3$-$PbTiO_3$ single crystals close to the morphotropic phase boundary

J. Peräntie,[1] J. Hagberg,[1] A. Uusimäki,[1] J. Tian,[2] and P. Han[2]
[1]*Microelectronics and Materials Physics Laboratories, University of Oulu, P.O. Box 4500, 90014 Oulu, Finland*
[2]*HC Materials Corporation, 479 Quadrangle Dr., Suite E, Bolingbrook, Illinois 60440, USA*

(Received 29 May 2012; accepted 17 July 2012; published online 10 August 2012)

The special characteristics of polarization rotation and accompanying electric-field-induced ferroelectric-ferroelectric phase transitions in ⟨001⟩-poled $Pb(Mg_{1/3}Nb_{2/3})_{1-x}Ti_xO_3$ ($x = 27.4$, 28.8, and 30.7 mol. %) single crystals close to the morphotropic phase boundary region were studied by means of dielectric and thermal measurements as a function of a unipolar electric field at various temperatures. Discontinuous first-order-type phase transition behavior was evidenced by distinct and sharp changes in polarization and thermal responses with accompanying hysteresis as a function of the electric field. All compositions of crystals showed either one or two reversible discontinuities along the polarization rotation paths, which can be understood by electric-field-induced phase transition sequences to the tetragonal phase through different monoclinic phases previously observed along the polarization rotation path. Together with increasing polarization, a field-induced reversible decrease in temperature was observed with increasing electric field, indicating increased dipolar entropy during the electric-field-induced phase transitions. Constructed electric field-temperature phase diagrams based on the polarization and thermal data suggest that the complex polarization rotation path extends to a wider composition range than previously observed. The measured thermal response showed that a transition from the monoclinic to the tetragonal phase produced a greater thermal change in comparison with a transition within two monoclinic phases. © *2012 American Institute of Physics*. [http://dx.doi.org/10.1063/1.4745902]

## I. INTRODUCTION

Large polarization changes in ferroelectric materials can lead to extraordinary enhancements in corresponding piezoelectric and other related properties. In particular, significant variation in polarization is introduced near regions where phase transitions are induced by various external means, such as an electric field or temperature.[1–3] Unusually high piezoelectric activity is found in complex perovskite single crystals of $Pb(Mg_{1/3}Nb_{2/3})_{1-x}Ti_xO_3$ (PMN-*x*PT) and $Pb(Zn_{1/3}Nb_{2/3})_{1-x}Ti_xO_3$ (PZN-*x*PT) close to the compositionally induced phase transition regions (i.e., the morphotropic phase boundary region), where they show one of the highest known piezoelectric coefficients, strains, and electromechanical coupling factors in non-polar directions.[4–6]

This peculiar electromechanical behavior is currently understood to be mainly caused by the ease of polarization rotation through different monoclinic phases considered to be structural bridges between higher symmetry phases.[3,7,8] A more universal approach to understanding enhanced intrinsic piezoelectricity is the idea of free-energy instability or flatness of the energy surface. A considerable dielectric anisotropy can be found in the vicinity of the phase transition regions, where a crystal is electromechanically softer in directions perpendicular to the initial spontaneous polarization. This leads to a flattening of the energy surface, a consequent ease of polarization rotation, and a large piezoelectric response in that direction.[9] Interestingly, and somewhat expectedly, these polarization rotation paths with free energy instabilities eventually lead to various electric-field-induced phase transitions in these materials.[5,9–11]

Generally, there are only very few phase diagrams constructed for single crystals of PMN-PT, especially under an applied electric field. Although the bulk polycrystalline system has been characterized more thoroughly, those results should be applied to poled crystals very carefully. Problems arise because of the near degeneracy of the different ferroelectric phases, which makes phase stability strongly dependent on the direction and strength of the applied electric field as well as on the method of poling.[12,13] However, it is well known that the PMN-PT material system, like many highly piezoelectric material systems in general, forms a morphotropic phase boundary (MPB) region, where rhombohedral and tetragonal phases meet with some lower symmetry monoclinic phases. Careful structural studies of the ceramic PMN-*x*PT system have shown that the low-temperature and zero-field phase diagram close to the MPB region starts from a rhombohedral R (point group 3*m*) phase and gradually develops into a tetragonal T (4*mm*) phase through monoclinic $M_B$ (*m*) and $M_C$ (*m*) phases with increasing *x*.[14–16] Otherwise, in single crystals of PMN-PT, as a side of the monoclinic $M_C$ phase, a monoclinic $M_A$ (*m*) phase has been evidenced in ⟨001⟩-poled (all indexes are expressed with respect to the cubic system) single crystals of PMN-

 

25PT, PMN-30PT, and PMN-35PT, and additional orthorhombic O (*mm*2) and monoclinic $M_B$ (*m*) phases have been detected with a ⟨011⟩-directed field.[17–19]

Of the most convenient {001}, {011}, and {111} crystallographic cuts, the {001} plate is the most studied, and it shows the highest $d_{33}$, strain, and mechanical coupling factor.[5,6] Previous structural analysis shows that an electric field applied in the ⟨001⟩ direction transforms a PMN-PT crystal from the rhombohedral phase to the tetragonal phase via different monoclinic $M_A$ and/or $M_C$ bridging phases, depending on the composition and temperature, quite similarly to other high-performance PZN-PT piezoelectric crystals.[10–12,17,20–22] To date, three distinct composition regions with different electric-field-induced phase transition behavior have been distinguished in the MPB region of PMN-*x*PT and PZN-*x*PT. With reasonably low $PbTiO_3$ content, away from the MPB region (approximately $x \leq 26\%$ for PMN-*x*PT), polarization of the rhombohedral R phase seems to rotate through the $M_A$ monoclinic phase to the tetragonal T phase with the application of a high enough ⟨001⟩-directed electric field.[10,20] In a narrow composition range, close to the rhombohedral side of the morphotropic phase boundary region, two different monoclinic phases of $M_A$ and $M_C$ type have been observed along the rotation pathway.[10,11,17,21] With an even higher PT concentration closer to the tetragonal side of the MPB region, only a monoclinic $M_C$ phase is found to be present in the rotation path.[12,22] Generally, it appears that a kind of crossover between two different electric-field-induced phase transition sequences, namely $M_A \rightarrow T$ and $M_C \rightarrow T$, takes place in a certain narrow $PbTiO_3$ concentration region in PMN-PT as well as in PZN-PT.

Accompanying clear jumps and hysteretic behavior in a macroscopic strain and/or polarization has been observed in all of the aforementioned rotation paths.[5,23–26] This clearly suggests the presence of some first-order-like phase transition characteristics. In particular, Davis *et al.*[24] found by converse piezoelectric measurements of PMN-30.5PT and PMN-31PT single crystals that the previously detected intermediate polarization rotation path $M_A \rightarrow M_C \rightarrow T$ involves two reversible first-order-like discontinuous phase transitions—one within the monoclinic phases and the other from the monoclinic phase to the tetragonal phase. By using the results from electric-field-induced strain measurements, they were also able to construct *E-T* phase diagram frames for various compositions of ⟨001⟩-oriented PMN-PT single crystals. In general, the electric-field-induced phase transitions in PMN-PT and related PZN-PT are covered with continuous rotation paths within the mirror planes of monoclinic phases, and accompanying first-order jumps introduce some discontinuities along these paths. Some of the above-mentioned phase transitions seem to have a somewhat limited or incomplete reversibility. In particular, transitions from the rhombohedral ground state can recover other phases after removal of an electric field.[10,17,21,22]

Observation of discontinuous changes in polarization and strain with accompanying hysteresis are indeed good indications of the first-order-like nature of the electric-field-induced phase transitions in PMN-PT. Since the first-order phase transition behavior involves latent heat, crystal temperature is either increased or decreased discontinuously under adiabatic conditions during the electric-field-induced phase transition with first-order-like characteristics. Observation of field-induced thermal behavior as a side of dielectric polarization during the phase transition provides additional information about the nature of the electric-field-induced phase transitions, and estimations of a possibly involved latent heat/enthalpy change can be made in different polarization rotation paths.

In this study, thermal response and polarization rotation behavior in PMN-*x*PT single crystals near the morphotropic phase boundary region were studied as a function of a ⟨001⟩-directed unipolar electric field at various temperatures. From this information, detailed electric field-temperature phase diagrams with hysteresis were plotted at low temperatures, and the order of the observed phase transitions is discussed. In addition, the thermal nature of the electric-field-induced phase transition and the magnitude of the enthalpy change were evaluated from the field-induced temperature responses.

## II. EXPERIMENTAL

$Pb(Mg_{1/3}Nb_{2/3})_{1-x}Ti_xO_3$ single crystals were grown using a modified Bridgman technique.[27] (001) crystal plates with different properties along the crystal growth direction were prepared. Dielectric properties were measured using a precision LCR meter (HP/Agilent 4284A). For polarization and temperature measurements, crystals were attached with polyimide tape to thin electrode wires inside a specific sample holder. A triangular electric field stimulus was supplied through the electrode wires by a function generator (Agilent 33120A) in connection with a high-voltage amplifier (Radiant RT6000HVA). Sample temperature was measured through a K-type thermocouple using a nanovoltmeter (Agilent 34420A). Polarization current was determined from the voltage measured across a known resistor with a multimeter (Agilent 34411A). All the above-mentioned measurements were performed at constant temperatures using a temperature furnace (Memmert UFP-400 and Espec SU-261). A polarizing microscope (Olympus BX51TF) was used for identification of crystal extinction angles under cross-polarized light at room temperature.

## III. RESULTS AND DISCUSSION

Figure 1 shows the dielectric constant (the real part of the relative permittivity, $\varepsilon_r$) and loss tangent (tan $\delta$) as a function of temperature for the studied PMN-PT compositions on zero-field heating in a frequency range of $10^2$–$10^4$ Hz. Before the measurement started on heating, the crystals were poled with an electric field of $E = 10\,\text{kV/cm}$ at 25 °C. Here, thermal depolarization temperature $T_d$ was used to evaluate *x* in PMN-*x*PT compositions, following the equation $x = (T_d + 59)/631$ ($T_d$ in centigrade), which is based on a wide collection of experimental data.[13] Three different crystal compositions close to the MPB region were studied. These crystals showed thermal depolarization temperatures of 114 °C, 123 °C, and 135 °C (see Figure 1), which refer to corresponding compositions of PMN-27.4%PT, PMN-28.8%PT,

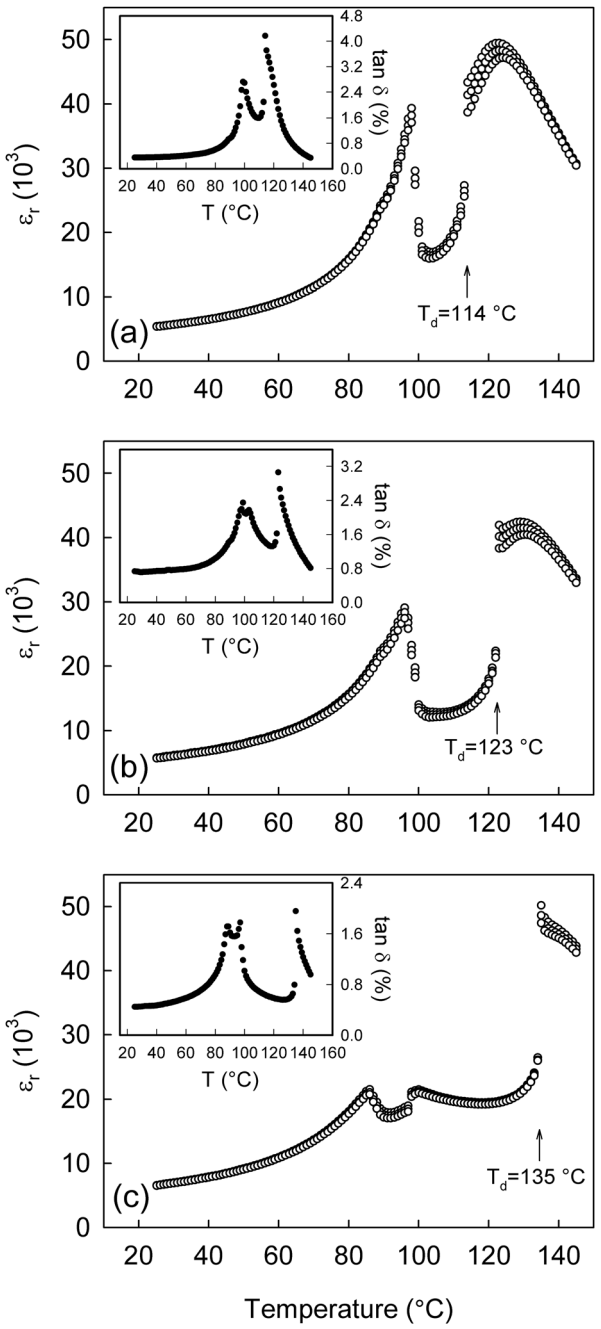


FIG. 1. Temperature dependence of the dielectric constant on heating for ⟨001⟩-poled (a) PMN-27PT, (b) PMN-29PT, and (c) PMN-31PT single crystals at 0.1, 1, and 10 kHz. Figure insets show temperature dependence of the loss tangent (tan $\delta$) at 1 kHz for corresponding crystal compositions.

and PMN-30.7%PT (from here on compositions values are rounded to the nearest integer percent).

In Figure 1(a)), a poled PMN-27PT crystal shows three distinct changes in its permittivity and loss tangent: first, a small peak at $T = 96\,^{\circ}\mathrm{C}$, then a second change at $T_d = 114\,^{\circ}\mathrm{C}$, and a third one at $T_m = 122$–$124\,^{\circ}\mathrm{C}$. Typical relaxation behavior is seen at temperatures around $T_m$, as expected. According to structural studies,[28] an unpoled PMN-27PT crystal is rhombohedral at room temperature. The crystals were also checked using polarized light microscopy (PLM) before poling, and extinctions in birefringent areas were found only with a polarizer at an angle of $\theta = 45°$ with respect to the ⟨001⟩ direction in the (001) plane. This indicates that the crystals are rhombohedral and poling into the ⟨001⟩ direction creates a domain-engineered 4R state or a distorted pseudo-rhombohedral monoclinic $4M_A$ state, which are practically indistinguishable by optical means in the (001) plane. On heating, this domain-engineered state transforms at 96 °C to a tetragonal phase with considerably lower permittivity. Thermal depolarization takes place at $T_d$, where the crystal changes from macroscopically polar to microscopically polar material with average cubic symmetry.

When $PbTiO_3$ concentration is increased (Figures 1(b) and 1(c)), related temperatures $T_d$ and $T_m$ move to higher temperatures and gradually converge towards a single sharp phase transition temperature at $T_C$. At the same time, the change at the first transition temperature splits into two distinct peaks. In PMN-29PT, a very small change in the permittivity slope appears just above the first peak at 103 °C, and this change is clearly evident in the corresponding loss curve (inset of Figure 1(b)). A higher PT concentration in PMN-31PT results in strengthening of the second peak, and it is clearly seen in both permittivity and loss tangent (Figure 1(c)). A very similar appearance of a double peak in temperature dependence of dielectric properties has been evidenced in ⟨001⟩-poled PMN-PT single crystals close to the MPB region.[26,29–33] Generally, an appearance of two peaks is only observed for crystals poled with high enough electric fields. This behavior is indeed attributed to the emergence of a new phase transition in the ⟨001⟩-poled sample at low temperatures and a narrow composition range. As previously shown for a ⟨001⟩-oriented PMN-30%PT crystal by means of x-ray and neutron diffraction,[17] isothermal application of an electric field at lower temperatures leads to polarization rotation and an accompanying phase transition sequence of $R \rightarrow M_A \rightarrow M_C \rightarrow T$, where the first transition exhibits an irreversible nature. A similar sequence can be considered here; the first transition takes place during poling and the remaining phase sequence is sequentially induced from pseudo-rhombohedral $R/M_A$ now by increasing temperature, as was shown in the permittivity and loss tangent curves for PMN-29PT and PMN-31PT. Additionally, the strength of the observed dielectric changes was found to exhibit great sensitivity to the poling electric field strength.

Furthermore, Figure 2 shows the behavior of the dielectric constant on heating and immediately repeated cooling between 25 and 115 °C for a poled ($E = 5$ kV/cm) PMN-31PT composition, which showed the most distinct changes in permittivity. This shows that considerable hysteresis is involved in both low-temperature phase transitions, $R/M_A \leftrightarrow M_C$ and $M_C \leftrightarrow T$. On heating the permittivity changes are observed at $T = 85\,^{\circ}\mathrm{C}$ and $T = 92\,^{\circ}\mathrm{C}$, while on cooling these changes take place at $T = 79\,^{\circ}\mathrm{C}$ and $T = 52\,^{\circ}\mathrm{C}$, correspondingly. The clear difference in the magnitudes of hysteresis between these phase transitions also suggests that they are indeed two separate transitions as a distinction from a possible single phase transition induced in two distinct steps within different parts of the crystal. However, it should be kept in mind that PMN-PT very likely has some phase coexistence as a function of temperature and field close to the

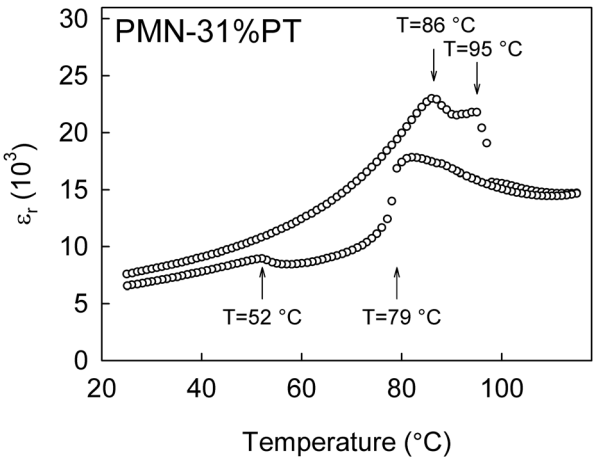


FIG. 2. Temperature dependence of the dielectric constant on heating and cooling for a ⟨001⟩-poled PMN-31PT single crystal at 1 kHz.

MPB region, as observed in many studies.[15,16,22,34–36] From this point of view, it is possible that separate regions of the crystal show different phase transitions of type $M_A \leftrightarrow T$ and $M_C \leftrightarrow T$, where coexistence of $M_A$ and $M_C$ phases would occur and no transition between monoclinic phases would take place. Actually, coexistence of $M_A$ and $M_C$ phases has been observed by PLM in an as-grown PMN-32PT crystal, but at the same time, it was discovered that a transition between monoclinic phases, namely $M_A \leftrightarrow M_C$, takes place on heating and cooling, and only the $M_A$ phase was stable after cooling.[35] Most likely some coexistence, where the other phase may be undetectable with many conventional probing techniques, is present due to both extrinsic and intrinsic factors, and therefore the assigned phases are considered to be major phases.

In order to study electric-field-induced behavior along polarization rotation paths, crystal temperature and polarization were recorded isothermally on cooling from 95 °C to 32 °C with a maximum unipolar electric field of 20 kV/cm. For each studied PMN-PT crystal composition, sharp reversible and simultaneous changes with hysteretic behavior in both polarization and temperature were observed (Figures 3 and 4). These are further indications of accompanying first-order-like characteristics in the corresponding electric-field-induced phase transitions along the otherwise continuous polarization rotation paths. According to the electric-field-induced polarization and temperature change behavior, three distinct low-temperature ranges with different behavior were identified (within the experimental conditions used) in these crystals. At high temperatures (but below $T_d$) poled crystals show low hysteresis and nearly linear temperature and polarization responses. Within this temperature range, all PMN-PT compositions are in the tetragonal phase, where increasing the field in the ⟨001⟩ direction drives the material towards a monodomain configuration. Below a specific temperature, a poled tetragonal crystal transforms to the monoclinic $M_C$ phase, which has polarization in a plane between the ⟨001⟩ and ⟨101⟩ polarization directions. This polarization can be induced back to the tetragonal phase with an increasing ⟨001⟩-directed electric field. Clear changes in polarization and temperature with accompanying hysteresis reaffirms that

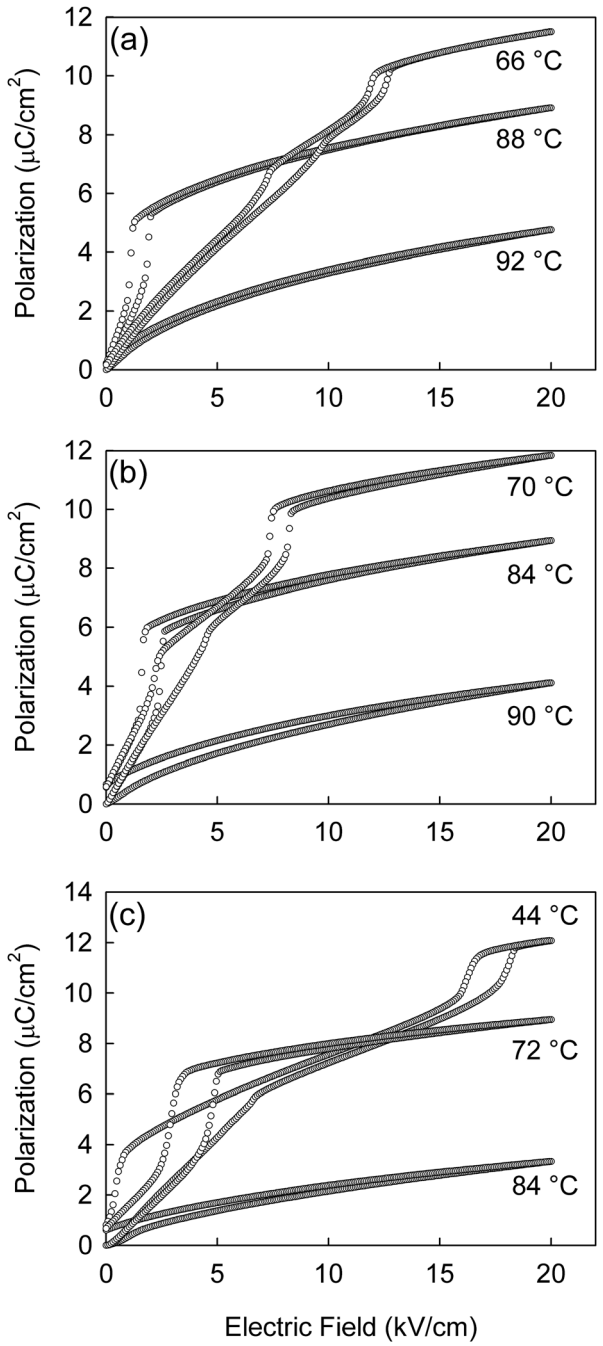


FIG. 3. Series of dielectric polarization loops for ⟨001⟩-poled (a) PMN-27PT, (b) PMN-29PT, and (c) PMN-31PT single crystals. Each curve was measured isothermally on cooling at fixed temperatures.

this electric-field-induced phase transition shows first-order-like characteristics. Another addition to the electric-field-induced phase transition sequence comes at lower temperatures, when a poled crystal transforms to another monoclinic phase, namely $M_A$. In this case, polarization rotates towards the tetragonal phase through two monoclinic phases, as indicated by structural studies.[17] Again, first-order-like jumps are found in both phase transitions. These changes in polarization show characteristics similar to strain-electric-field measurements performed for ⟨001⟩-poled PMN-PT crystals.[24,26]

In general, application of an electric field in the ⟨001⟩ direction causes polarization to continuously rotate towards

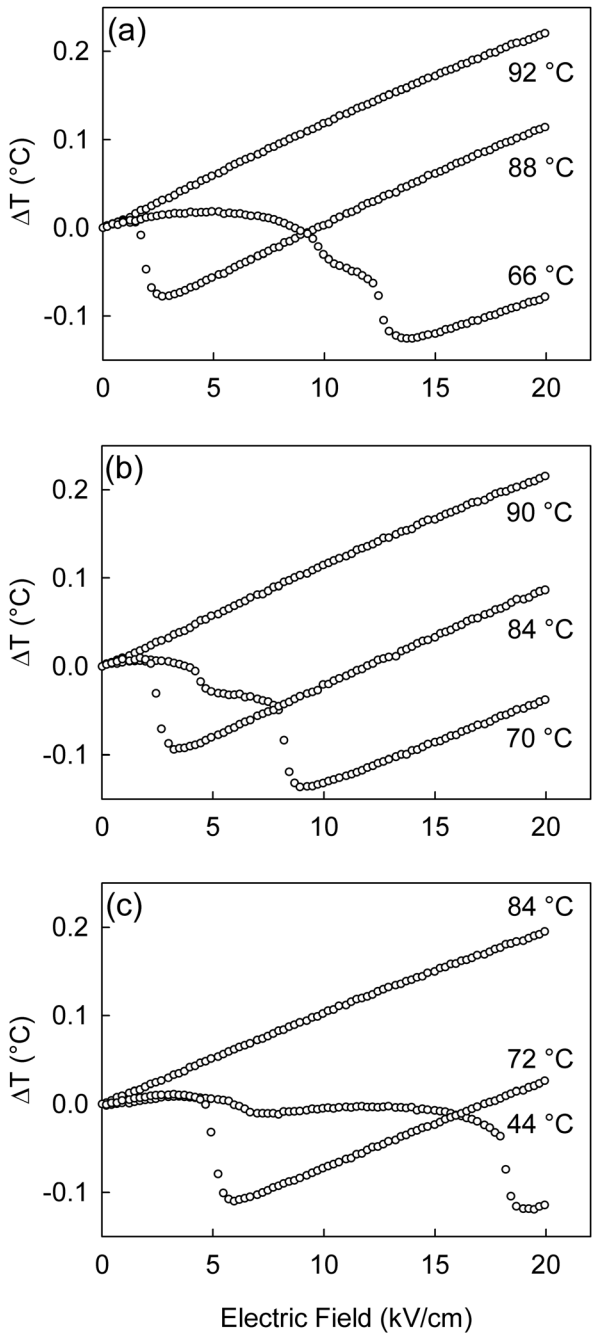


FIG. 4. Series of *in-situ* temperature responses with an increasing electric field measured from the crystal surface during unipolar polarization measurement for ⟨001⟩-poled (a) PMN-27PT, (b) PMN-29PT, and (c) PMN-31PT single crystals.

that direction. This, in turn, leads to a change in the material's dipolar entropy ($\Delta S_{dip}$) due to alignment of dipoles. Under adiabatic conditions ($\Delta S_{tot} = 0$), a change in dipolar entropy must be compensated by other entropy contributions, such as a phonon-related entropy change, which cause temperature to change. Then, at certain points the temperature of the crystal decreases in a more discontinuous manner due to electric-field-induced phase transitions evidenced also in polarization measurements. A sudden temperature decrease means that dipolar entropy is temporarily increased with the electric field (i.e., $(\partial S_{dip}/\partial E)_T > 0$), and heat is absorbed (Figure 4). Similar behavior was also evidenced experimentally in PMN-PT close to room temperature with a ⟨011⟩-directed electric field.[37] Furthermore, atomistic simulations on $(Ba,Sr)TiO_3$ reproduced similar characteristics with a negative temperature change when an electric field was applied in the non-polar direction.[38] This behavior is reversed when the electric field starts to decrease, and corresponding temperature changes are observed at lower electric fields. Interestingly, the crystal temperature started to change slowly already before each more rapid change during the transitions. This diffuse behavior emerged especially with higher threshold electric fields, where both transitions were observed along the polarization rotation path, and it was generally found to be independent of the rate of field change. Especially in a $M_C$-T-type transition, the difference between more continuous- and discontinuous-like parts within the temperature responses was recognized, and the overall temperature change was in the range of 97-136 mK. However, quantitative discrimination between the continuous and discontinuous parts proved to be complicated. The other M-M-type transition showed smaller temperature changes with even more diffuse characteristics, but still clear hysteresis similar to polarization measurements was observed between the inducing threshold electric fields. These observations were in line with the polarization measurements, where highly diffuse characteristics were also observed in the M-M-type transition, especially with an increasing field (Figure 3). Similar diffuse behavior has also been evidenced in strain-electric field measurements.[13,24] Characteristic random fields in relaxors have been suggested to induce this type of diffuse behavior by variation of threshold fields,[39] and similar variation can be expected also from Ti-concentration variations. Otherwise, crystals showing weak first-order phase transition characteristics have smaller discontinuous latent heat and show continuous/diffuse behavior. Weakly first-order phase transitions with critical behavior have been found to take place in a PMN-PT crystal, especially with a biasing electric field.[40,41] Additionally, it has to be pointed out that some heat exchange takes place between the sample and its surroundings due to the considerably slow rise time (10 s) of the electric field. The measured thermal time constant of the sample showed values close to 60 s. However, qualitatively the behavior remained similar also with faster rise times, and a slower rise time was only used to get a sufficient amount of measurement points to determine the threshold field strengths. Generally, temperature responses were found to be closely reversible, although involved hysteresis loss and heat leakage had a very small but compensating influence on the response.

Based on measured temperature and polarization changes, threshold electric fields for electric-field-induced phase transitions were acquired and corresponding electric field vs. temperature phase diagrams were plotted in Figure 5. As mentioned earlier, all PMN-PT compositions showed a temperature region which involved two reversible polarization and temperature discontinuities along the polarization rotation route, and thus point to the electric-field-induced phase transition sequence of $M_A \rightarrow M_C \rightarrow T$ with an increasing field. To date, this phase transition sequence at constant temperatures has been discovered by diffraction techniques

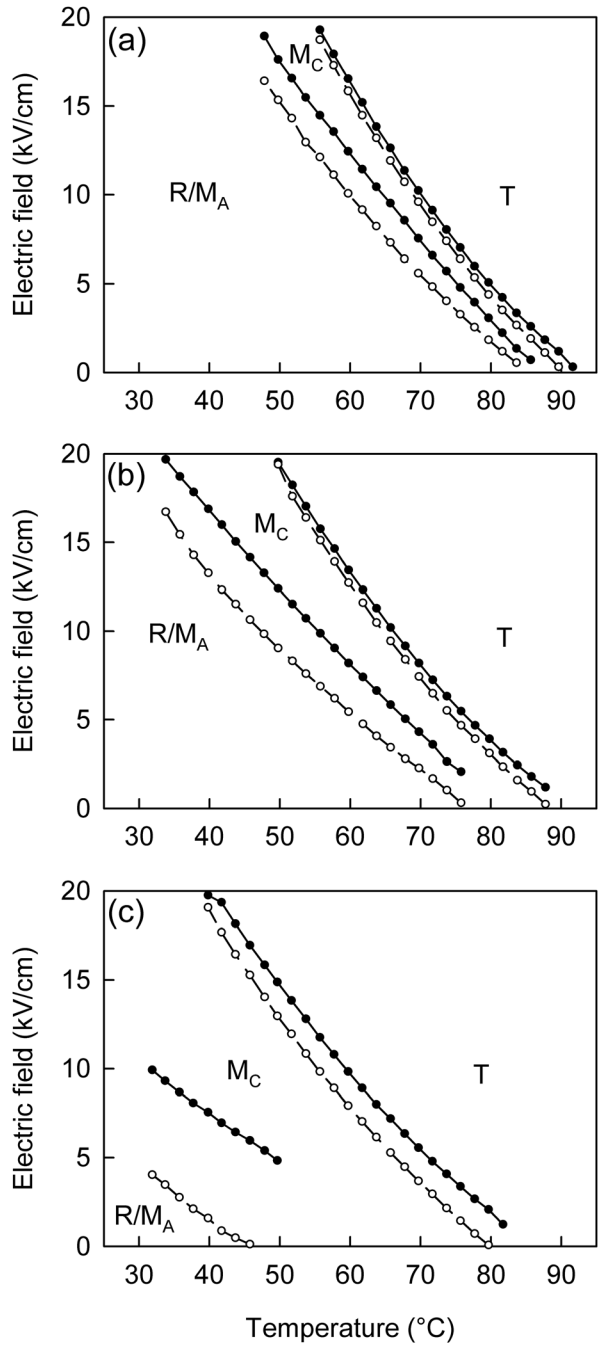


FIG. 5. Electric field-temperature diagrams showing locations of measured discontinuities in field-induced isothermal polarization and temperature with an increasing/decreasing electric field for ⟨001⟩-poled (a) PMN-27PT, (b) PMN-29PT, and (c) PMN-31PT single crystals. Black (white) circles indicate threshold field strengths with an increasing (decreasing) electric field.

only in a PMN-$x$PT composition with $x = 30\%$ (and additionally in PZN-8PT).[10,17,21] The majority of other earlier studies on electric-field-induced phase transitions in ⟨001⟩-oriented PMN-PT single crystals have been performed by heating and/or cooling with constant electric fields, and this approach most likely gives somewhat different results in comparison with applying an electric field at constant temperature. For instance, using high-resolution diffraction studies, Cao *et al.*[12] have found a phase sequence of C → T → $M_A$ on field-cooling (FC) with $E_{\langle 001\rangle} = 0.5$ kV/cm in PMN-27PT and PMN-28PT single crystals, but no sign of a $M_C$ phase was found. Only an intermediate PMN-30PT composition, like in the case of isothermal electric field application, showed two monoclinic phases in the FC phase sequence of C → T → $M_C$ → $M_A$, and a higher $PbTiO_3$ concentration in PMN-32PT and PMN-35PT returned a phase sequence of C → T → $M_C$ during the FC routine.[12,42,43] This clearly shows that the complex rotation path with two monoclinic phases is very sensitive to $PbTiO_3$ concentration. One reason for the absence of another monoclinic phase in field-cooled PMN-$x$PT with $x \neq 30\%$ in these studies could be the use of limited experimental conditions. Otherwise, it is possible that cooling with a constant electric field would more easily destroy the near degeneracy of phases locking the other lower-energy phase in place, and no transition between two monoclinic rotation planes would take place anymore at lower temperatures. However, polarization rotations with two distinct discontinuities, implying the previously found $M_A \leftrightarrow M_C \leftrightarrow T$ reversible phase transition sequence, have also been evidenced indirectly with isothermal strain-electric field measurements in ⟨001⟩-oriented PMN-$x$PT compositions with $x > 30\%$.[24] This suggests that the monoclinic $M_A$-type phase instead of the $M_C$ phase is the stable ground phase for ⟨001⟩-poled crystals also with $x$ slightly above 30%. Somewhat analogous results have been obtained in refinement of the zero-field phase diagram of polycrystalline PMN-$x$PT system, where the $M_B$ phase seems to lie close to the $M_C$ phase.[16,44] Critically, the existence of both ferroelectric monoclinic $M_A$ and $M_C$ phases in ⟨001⟩-poled PMN-$x$PT crystals also with $x \geq 30\%$ has been previously reported.[17,18,45] It seems that at some point in the MPB region, the major metastable monoclinic $M_C$ phase can be induced irreversibly with a high enough poling field, which also leads to a degradation of piezoelectric properties—a process commonly called overpoling.[46,47] Based on measured dielectric and thermal results in combination with some of the aforementioned earlier results, it is assumed that the PMN-$x$PT crystal compositions studied herein ($x = 27$–31 mol. %) are all macroscopically in the $M_A$ major phase after ⟨001⟩ poling at room temperature, since they all show two reversible discontinuities pointing to distinct electric-field-induced phase transitions with some first-order characteristics. More structural studies, especially on single crystals under an applied electric field, are still needed to form a more complete picture of their evidently fragile phase stability.

The observed phase transitions in a ⟨001⟩-poled PMN-27PT crystal occurred very close to each other, and the stability region of the monoclinic $M_C$ phase proves to be very narrow (Figure 5(a)). Thus, this crystal composition lies in close proximity to a critical $PbTiO_3$ concentration above which a new phase transition and polarization rotation sequence emerges with an additional first-order-like jump between two monoclinic rotational planes. Although a small stability range of the $M_C$ phase can be seen for PMN-27PT in polarization measurements on cooling, it is not evident in the dielectric constant measurements on heating (Figure 1(a)). With increasing $PbTiO_3$ concentration, the stability region of the $M_C$ phase gradually increases at the expense of the $M_A$ phase region in a very similar manner as previously

found with field-induced strain measurements.[24] At the same time, the magnitude of hysteresis ($E_{incr}$–$E_{decr}$) in the phase transition shows a drastic increase with increasing $x$, especially for $M_A \leftrightarrow M_C$ phase transition. Concomitantly decreasing phase transition threshold fields show a general trend of $M_C$ phase stabilization with even higher $PbTiO_3$ concentrations, where it is first stabilized by irreversible overpoling and finally it develops spontaneously with a further increase of $x$. Additionally, transition temperatures found on cooling for PMN-31PT in Figure 2 are in reasonably good agreement with temperatures found in Figure 5(c) for decreasing threshold electric fields. The stability regions depicted in Figure 5 are also plotted as a function of the studied composition in Figure 6 for electric fields of 0 and 4 kV/cm. The values were taken with a decreasing electric field at constant temperatures, and a trend for $M_C$ phase stabilization is clearly seen. This figure resembles the modified phase diagram sketched earlier by Cao *et al.* (Figure 1 in Ref. 42), where a vertical phase boundary line close to the MPB in the $T$-$x$ phase diagram starts to turn towards a lower $x$ at higher temperatures.

Finally, all the field-induced thermal responses were analyzed in more detail, and the magnitudes of total temperature drops for each related phase transition were extracted from otherwise nearly linear responses. The values were taken with a decreasing electric field due to more distinct changes. Some data close to either phase transition region or experimental boundary were unclear and omitted. All the temperature changes were further transformed to give corresponding specific enthalpy changes $\Delta H$ ($=c_p \Delta T$), assuming nearly adiabatic conditions and a constant specific heat capacity ($c_p \sim 0.32$ J/gK)[48] for all compositions. The total specific enthalpy changes (total drop in temperature) in $M_A$-$M_C$- and $M_C$-T-type phase transitions were in the range of 8–18 mJ/g and 30–44 mJ/g depending on the composition and temperature (Figure 7). The enthalpy change of the M-M-type transition decreased with increasing $x$, while the corresponding values for the M-T-type transition showed opposite behavior. Notably, a very similar enthalpy change value of 35 mJ/g (in the $E=0$ plane) was measured by high-resolution calorimetry on cooling for a similar T-$M_C$-type transition in a ⟨111⟩-poled PMN-29.5PT single crystal.[40,49] However, comparison of a.c. and relaxation calorimetry modes revealed that the specific latent heat $L$ related to the T-$M_C$ transition was approximately less than 10 mJ/g (even in the $E=0$ plane),[49] which is significantly smaller than the total enthalpy change $\Delta H$. This indicates that a continuous part of the enthalpy change $\delta H$ plays a significant role, and the transition itself shows signs of a weak first-order phase transition. When the electric field was increased, it was also discovered that the latent heat gradually disappeared, and the total enthalpy change decreased to 4 mJ/g at the critical end point.[40,49] However, in our measurements with a ⟨001⟩-directed field, a larger part of the temperature changed sharply, implying a larger latent heat. Additionally, in this study, the increasing ⟨001⟩-directed electric field tended to stabilize the high-temperature tetragonal phase at lower temperatures (Figure 5).

Interestingly, Kutnjak *et al.*[40,41,49] also observed the critical end point in a high-temperature C-T phase transition as well as in several ferroelectric-ferroelectric phase transitions (including the mentioned T-$M_C$ transition line) when an increasing electric field was applied in the ⟨110⟩ and ⟨111⟩ directions. At the critical end point, the line of first-order

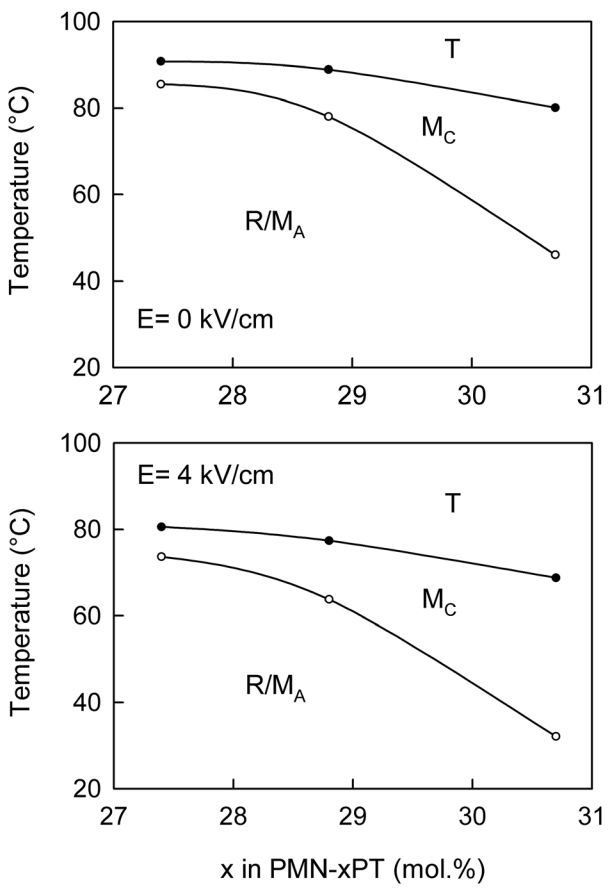


FIG. 6. Phase stability regions in ⟨001⟩-poled PMN-$x$PT single crystals for electric fields of 0 and 4 kV/cm. The values extracted from the polarization response to isothermally applied electric fields on cooling.

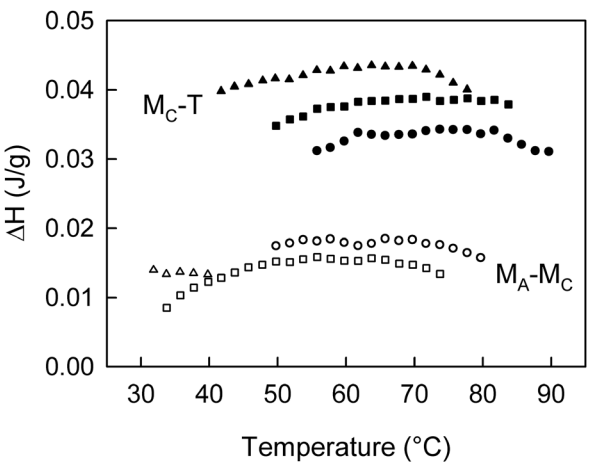


FIG. 7. Specific enthalpy change values from corresponding temperature changes measured for two distinct electric-field-induced phase transitions of $M_A$-$M_C$ and $M_C$-T. The temperature change values were taken with a decreasing electric field. Different symbols are used to indicate different single crystal compositions of PMN-27PT (circles), PMN-29PT (squares), and PMN-31PT (triangles).

phase transitions terminates, latent heat vanishes, and supercritical broad response anomalies without the phase transition are observed beyond that point.[40] No corresponding critical point has been found in the cubic-rhombohedral phase transition with $E\|\langle 001\rangle$ for PMN,[50,51] but signs of its existence have been observed in high-temperature phase transitions of $\langle 001\rangle$-oriented PMN-$x$PT compositions.[52] In this study, the lower-temperature $M_C$-T phase transition line showed first-order-like anomalies and hysteresis within the measurement range. However, a closer look at the temperature responses indicated that the accompanying discontinuous part showed weakly decreasing values when higher electric fields were required for the phase transition. At the same time, the amount of hysteresis and the rate of polarization change also showed a slight decrease. These observations imply an accompanying continuous nature and weakening first-order part in the phase transitions. Otherwise, a possible critical end point (if any) may appear with higher fields, but definitive signs of its emergence could not be determined here for this transition based on our measurement data and range. Indeed, the critical end point can also be hidden and not attainable in first-order lower-temperature transitions.[53] Additionally, the first-order-like phase transition between monoclinic phases showed even more diffuse characteristics in both polarization and temperature change, but considerable hysteresis was also involved. Notably, the combined amount of total field-induced temperature decrease measured here with $E\|\langle 001\rangle$ was found to be significantly larger than in a similar PMN-PT crystal with $E\|\langle 011\rangle$.[37]

## IV. SUMMARY AND CONCLUSIONS

Polarization rotation in $\langle 001\rangle$-poled single crystals of PMN-$x$PT close to the morphotropic phase boundary region ($x = 27.4$, 28.8, and 30.7 mol. %) was studied by means of dielectric and temperature measurements. Low-temperature electric-field-induced discontinuities, in particular, were taken under more detailed investigation.

All the studied compositions showed either one or two reversible discontinuous first-order-like changes with hysteretic behavior in polarization and temperature as a response to a unipolar electric field at constant temperatures. The observed changes were attributed to two reversible electric-field-induced phase transition sequences of $M_A \leftrightarrow M_C$ and $M_C \leftrightarrow T$, which have been evidenced earlier by diffraction techniques for PMN-PT compositions with $E$ parallel to $\langle 001\rangle$. Crystal temperature was decreased during both field-induced phase transitions, which indicates an increase in field-induced dipolar entropy. Extracted temperature changes were significantly smaller in the M-M-type transition, and despite the presence of clear hysteresis, the observed field-induced changes showed considerable diffuse/continuous behavior, depending on the temperature and composition.

Based on the measurement results, $E$-$T$ phase diagrams were plotted for poled PMN-$x$PT compositions, and the complex polarization rotation path extended to a wider composition range than previously observed. Otherwise, the regions assigned to the $M_C$ and T phases were found to stabilize at lower temperatures with increasing $PbTiO_3$ concentration and electric field.

From a practical point of view, the results of this work show that the total reversible temperature change $\Delta T$ (i.e., electrocaloric effect) may include competing effects (negative and positive), which degrade the magnitude of the total entropy change and electrocaloric effect. Critically, this is rarely an issue in practice, since the maximum electrocaloric effect with potential application interest is achieved close to the nonpolar-polar phase transition, where electric-field-induced contributions tend to decrease dipolar entropy. On the other hand, it has been suggested that a controlled combination of positive and negative electrocaloric effects could lead to increased cooling cycle efficiency.[38]

## ACKNOWLEDGMENTS

J.P. gratefully acknowledges the Graduate School in Electronics, Telecommunications and Automation (GETA), the Nokia Foundation, the Jenny and Antti Wihuri Foundation, the Tauno Tönning Foundation, the Ulla Tuominen Foundation, the Riitta and Jorma J. Takanen Foundation, the Seppo Säynäjäkangas Science Foundation, the Kaute Foundation, and the Finnish Cultural Foundation for the financial support of this work.

[1]D. Damjanovic, Appl. Phys. Lett. **97**, 062906 (2010).
[2]M. Budimir, D. Damjanovic, and N. Setter, J. Appl. Phys. **94**, 6753 (2003).
[3]H. Fu and R. E. Cohen, Nature **403**, 281 (2000).
[4]T. R. Shrout, Z. P. Chang, N. Kim, and S. Markgraf, Ferroelectr., Lett. Sect. **12**, 63–69 (1990).
[5]S.-E. Park and T. R. Shrout, J. Appl. Phys. **82**, 1804 (1997).
[6]S.-E. E. Park and W. Hackenberger, Curr. Opin. Solid State Mater. Sci. **6**, 11 (2002).
[7]B. Noheda, Curr. Opin. Solid State Mater. Sci. **6**, 27 (2002).
[8]B. Noheda and D. E. Cox, Phase Transitions **79**, 5 (2006).
[9]D. Damjanovic, IEEE Trans. Ultrason. Ferroelectr. Freq. Control **56**, 1574 (2009).
[10]B. Noheda, Z. Zhong, D. E. Cox, G. Shirane, S.-E. Park, and P. Rehrig, Phys. Rev. B **65**, 224101 (2002).
[11]B. Noheda, D. E. Cox, G. Shirane, S.-E. Park, L. E. Cross, and Z. Zhong, Phys. Rev. Lett. **86**, 3891 (2001).
[12]H. Cao, J. Li, D. Viehland, and G. Xu, Phys. Rev. B **73**, 184110 (2006).
[13]M. Davis, Ph.D. dissertation, Ecole Polytechnique Federale de Lausanne (EPFL), 2006.
[14]J.-M. Kiat, Y. Uesu, B. Dkhil, M. Matsuda, C. Malibert, and G. Calvarin, Phys. Rev. B **65**, 064106 (2002).
[15]B. Noheda, D. E. Cox, G. Shirane, J. Gao, and Z.-G. Ye, Phys. Rev. B **66**, 054104 (2002).
[16]A. K. Singh and D. Pandey, Phys. Rev. B **67**, 064102 (2003).
[17]F. Bai, N. Wang, J. Li, D. Viehland, P. M. Gehring, G. Xu, and G. Shirane, J. Appl. Phys. **96**, 1620, (2004).
[18]Z.-G. Ye, B. Noheda, M. Dong, D. Cox, and G. Shirane, Phys. Rev. B **64**, 184114 (2001).
[19]H. Cao, F. Bai, N. Wang, J. Li, D. Viehland, G. Xu, and G. Shirane, Phys. Rev. B **72**, 064104 (2005).
[20]R. R. Chien, V. H. Schmidt, C.-S. Tu, L.-W. Hung, and H. Luo, Phys. Rev. B **69**, 172101 (2004).
[21]K. Ohwada, K. Hirota, P. W. Rehrig, Y. Fujii, and G. Shirane, Phys. Rev. B **67**, 094111 (2003).
[22]F. Fang, X. Luo, and W. Yang, Phys. Rev. B **79**, 174118 (2009).
[23]M. K. Durbin, E. W. Jacobs, J. C. Hicks, and S.-E. Park, Appl. Phys. Lett. **74**, 2848 (1999).
[24]M. Davis, D. Damjanovic, and N. Setter, Phys. Rev. B **73**, 014115 (2006).
[25]W. Ren, S.-F. Liu, and B. K. Mukherjee, Appl. Phys. Lett. **80**, 3174 (2002).

[26]F. Li, S. Zhang, Z. Xu, X. Wei, J. Luo, and T. R. Shrout, J. Appl. Phys. **108**, 034106 (2010).
[27]P. Han, J. Tian, and W. Yan, "Bridgman growth and properties of PMN-PT-based single crystals," in *Handbook of Advanced Dielectric, Piezoelectric, and Ferroelectric Materials—Synthesis, Properties and Applications*, edited by Z.-G. Ye (Woodhead, Cambridge, 2008), pp. 3–37.
[28]G. Xu, D. Viehland, J. F. Li, P. M. Gehring, and G. Shirane, Phys. Rev. B **68**, 212410 (2003).
[29]Y. Guo, H. Luo, D. Ling, H. Xu, T. He, and Z. Yin, J. Phys. Condens. Matter **15**, L77 (2003).
[30]C.-S. Tu, R.-R. Chien, F.-T. Wang, V. H. Schmidt, and P. Han, Phys. Rev. B **70**, 220103 (2004).
[31]Z. Feng, X. Zhao, and H. Luo, J. Appl. Phys. **100**, 024104 (2006).
[32]A. Slodczyk, Ph. Colomban, and M. Pham-Thi, J. Phys. Chem. Solids **69**, 2503 (2008).
[33]D. Lin, Z. Li, S. Zhang, Z. Xu, and X. Yao, J. Appl. Phys. **108**, 034112 (2010).
[34]Z.-G. Ye and M. Dong, J. Appl. Phys. **87**, 2312 (2000).
[35]P. Bao, F. Yan, X. Lu, J. Zhu, H. Shen, Y. Wang, and H. Luo, Appl. Phys. Lett. **88**, 092905 (2006).
[36]Y. Jiang, D. Fang, S. Hui, H. Luo, and Q. Yin, Acta Mater. **55**, 5614 (2007).
[37]J. Peräntie, J. Hagberg, A. Uusimäki, and H. Jantunen, Phys. Rev. B **82**, 134119 (2010).
[38]I. Ponomareva and S. Lisenkov, Phys. Rev. Lett. **108**, 167604 (2012).
[39]A. J. Bell, Appl. Phys. Lett. **76**, 109 (2000).
[40]Z. Kutnjak, J. Petzelt, and R. Blinc, Nature **441**, 956 (2006).
[41]Z. Kutnjak, Ferroelectrics **369**, 198 (2008).
[42]H. Cao, F. Bai, J. Li, D. Viehland, G. Xu, H. Hiraka, and G. Shirane, J. Appl. Phys. **97**, 094101 (2005).
[43]H. Cao, J. Li, D. Viehland, G. Xu, and G. Shirane, Appl. Phys. Lett. **88**, 072915 (2006).
[44]A. K. Singh, D. Pandey, and O. Zaharko, Phys. Rev. B **74**, 024101 (2006).
[45]A. A. Bokov and Z.-G. Ye, Phys. Rev. B **66**, 094112 (2002).
[46]K. K. Rajan, M. Shanthi, W. S. Chang, J. Jin, and L. C. Lim, Sens. Actuators, A **133**, 110 (2007).
[47]A. A. Bokov and Z.-G. Ye, Appl. Phys. Lett. **92**, 082901 (2008).
[48]Y. Tang, X. Zhao, X. Feng, W. Jin, and H. Luo, Appl. Phys. Lett. **86**, 082901 (2005).
[49]Z. Kutnjak, R. Blinc, and Y. Ishibashi, Phys. Rev. B **76**, 104102 (2007).
[50]X. Zhao, W. Qu, X. Tan, A. A. Bokov, Z.-G. Ye, Phys. Rev. B **75**, 104106 (2007).
[51]Z. Kutnjak, B. Vodopivec, and R. Blinc, Phys. Rev. B **77**, 054102 (2008).
[52]S. I. Raevskaya, A. S. Emelyanov, F. I. Savenko, M. S. Panchelyuga, I. P. Raevski, S. A. Prosandeev, E. V. Colla, H. Chen, S. G. Lu, R. Blinc, Z. Kutnjak, P. Gemeiner, B. Dkhil, and L. S. Kamzina, Phys. Rev. B **76**, 060101 (2007).
[53]M. Iwata, Z. Kutnjak, Y. Ishibashi, and R. Blinc, J. Phys. Soc. Jpn. **77**, 034703 (2008).